



UNIVERSITÀ POLITECNICA DELLE MARCHE
Repository ISTITUZIONALE

Center of pressure plausibility for the double-link human stance model under the intermittent control paradigm

This is the peer reviewed version of the following article:

Original

Center of pressure plausibility for the double-link human stance model under the intermittent control paradigm / Tigrini, A.; Verdini, F.; Fioretti, S.; Mengarelli, A.. - In: JOURNAL OF BIOMECHANICS. - ISSN 0021-9290. - STAMPA. - 128:(2021). [10.1016/j.jbiomech.2021.110725]

Availability:

This version is available at: 11566/291953 since: 2024-04-25T09:37:10Z

Publisher:

Published

DOI:10.1016/j.jbiomech.2021.110725

Terms of use:

The terms and conditions for the reuse of this version of the manuscript are specified in the publishing policy. The use of copyrighted works requires the consent of the rights' holder (author or publisher). Works made available under a Creative Commons license or a Publisher's custom-made license can be used according to the terms and conditions contained therein. See editor's website for further information and terms and conditions.

This item was downloaded from IRIS Università Politecnica delle Marche (<https://iris.univpm.it>). When citing, please refer to the published version.

(Article begins on next page)

Center of Pressure Plausibility for the Double-Link Human Stance Model Under the Intermittent Control Paradigm

Andrea Tigrini^a, Federica Verdini^a, Sandro Fioretti^a, Alessandro Mengarelli^{a,*}

^a*Department of Information Engineering, Università Politecnica delle Marche, 60131, Ancona, Italy*

Abstract

Despite human balance maintenance in quiet conditions could seem a trivial motor task, it is not. Recently, the human stance was described through a double link inverted pendulum (DIP) actively controlled at the ankle with an intermittent proportional (P) and derivative (D) control actions based on the sway of a virtual inverted pendulum (VIP) that links the ankle joint with the DIP center of mass. **Such description, encompassing both the mechanical model and the intermittent control policy, was referred as the DIP/VIP human stance model, and it showed physiologically plausible kinematic patterns. In this study a mathematical formalization of the Center of pressure (COP) for a DIP structure was developed. Then, it was used in conjunction with an intermittently controlled DIP/VIP model to assess its kinetic plausibility.** Three descriptors commonly employed in posturography were selected among six based on their capability to discriminate between young (Y) and elderly (O) adults groups. Then, they were applied to assess whether variations of the P-D parameters affect the synthetic COP. The results showed that DIP/VIP model can reproduce COP trajectories, showing characteristics similar to the Y and O groups.

*Corresponding author

Email addresses: a.tigrini@pm.univpm.it (Andrea Tigrini), f.verdini@staff.univpm.it (Federica Verdini), s.fioretti@staff.univpm.it (Sandro Fioretti), a.mengarelli@pm.univpm.it (Alessandro Mengarelli)

Moreover, it was observed that both P and D parameters increased passing from Y to O, indicating that the COP obtained from the DIP/VIP model is able to highlight differences in balance control between groups. The study hence promote the use of DIP/VIP in posturography, where inferential techniques can be applied to characterize neural control.

Keywords: Center of pressure, Upright stance modeling, Human balance maintenance, Intermittent control

Word count:

3493

1. Introduction

The study of the human stance received close attention over the years, from biomechanics to neuroscience and robotics (Collins & De Luca, 1993; Peterka, 2000; Popović, 2013), focusing on the comprehension on how the Central Nervous System (CNS) manages the sensory information and how it generates control commands to stabilize the body, eventually preventing falls. Indeed, as experimentally demonstrated, ankle stiffness is not sufficient to guarantee the upright stance stability *per se* (Morasso & Sanguineti, 2002). Thus, a CNS mediated action must come into play to actively support the passive stabilizing mechanisms (Casadio et al., 2005; Baratto et al., 2002; Morasso et al., 2019).

The modeling of the human balance maintenance can be thereby viewed as a cybernetic problem, where the mechanics of the body affects and coexists with the processes that CNS is engaged to solve, i.e. sensory information fusion, motor commands generation and delivery (Morasso et al., 2019). Single-link (SIP) or double-link inverted (DIP) pendulum were commonly adopted to model the body stance (Morasso et al., 2019; Asai et al., 2009; Suzuki et al., 2012; Cenciarini et al., 2010), while the description of the neural controller is currently a discussed topic (Morasso et al., 2019). Many authors approached the problem through a continuous control paradigm, where proportional (P) and derivative (D) controllers act upon a delayed information of the sway angle (Peterka, 2000). This paradigm however presented some limitations, since it is highly sensitive to the feedback loop delay, with poor robust performances. From the other side, the idea that the CNS tunes the regulatory commands (Collins & De Luca, 1993) was further developed and proposed under the variable structure control (VSC) paradigm (Asai et al., 2009; Suzuki et al., 2012; Milton & Insperger, 2019). The latter constitutes a physiologically plausible alternative to a continuous control: through a VSC, the unstable sub-dynamics of the system can be stabilized

switching opportunely among them (Asai et al., 2009).

The model proposed by (Morasso et al., 2019) seemed to present a valuable synthesis of the human-balance maintenance. Indeed, the authors modeled the stance through a DIP structure on the sagittal plane, while the neural controller acts at the ankle with an intermittent control policy (Morasso et al., 2019; Asai et al., 2009). The hip instead contributes passively to the stabilization by over-stiffening the upper trunk (Morasso et al., 2019). A crucial point was the idea that CNS employs a delayed knowledge of the Center of Mass (COM) sway to generate active motor commands, leading to the use of a virtual inverted pendulum (VIP) that links the ankle joint to the COM, computed by the position of the DIP structure. Such model showed kinematic coordination patterns between the lower and the upper segments in line with those observed in human balancing (Morasso et al., 2019; Aramaki et al., 2001), resembling actual COM sway. However, no information was provided regarding the Center of Pressure (COP) fluctuations, which together with the COM play a key role in any quiet balancing task (Morasso, 2020). It should be emphasized that the COP time course is a directly measurable quantity, while COM can be only estimated through many possible procedures (Morasso et al., 1999; Cardarelli et al., 2019). Further, classical posturography recognizes COP as fundamental to extract useful information regarding how CNS regulates the stance through the control torques (Collins & De Luca, 1993; Baratto et al., 2002). COP accounts for the resultant control actions exerted not only at the ankle joint but also at the hip. Thus, a SIP model can provide only a limited mechanical description of the human stance.

In this work, a mathematical formulation of COP in the anterior-posterior direction for the DIP model was derived. Then, it was used to assess the plausibility of the DIP/VIP model in reproducing human-like COP balancing patterns,

relying on a set of suitable metrics, which require only the anterior-posterior component for their computation. The latter were selected using actual COP data, as descriptive of the underlying mechanisms behind CNS posture regulation (Amoud et al., 2007; Yamamoto et al., 2015; Collins & De Luca, 1993). The active controller parameters of the DIP/VIP were varied within a certain range of values (Morasso et al., 2019). The simulated COP were compared, according to the aforementioned metrics, with actual COP data belonging to two populations, i.e. young and elderly adults, where clear differences in sway patterns were expected.

2. Methods

2.1. Dataset presentation

Posturographic data of thirty healthy subjects from a public dataset were used (Santos & Duarte, 2016), fifteen belonging to a healthy adults group, representing a young cohort (Y) with an age not greater than 36.9 years and fifteen to an elderly group (O), presenting an age greater than 60.0 years. Data were sampled at 100 Hz for 60 s and filtered at 10 Hz with a zero-phase second order low-pass filter and detrended. Only the anterior-posterior component (AP) of COP was considered for further analysis since the DIP/VIP model describes upright posture in the sagittal plane.

2.2. DIP/VIP human upright stance model

The DIP/VIP model describes the human posture through a double link inverted pendulum (see figure 1). Its dynamic equations can be obtained by using the lagrangian formulation (Siciliano et al., 2010; Morasso et al., 2019). The two generalized coordinates q_1 and q_2 (see the appendix) represent the angles between the lower body segment and the vertical axis, and between the lower and upper body segments respectively.

Given $\mathbf{q} = \begin{bmatrix} q_1 & q_2 \end{bmatrix}^T$ one can obtain:

$$\begin{cases} \mathbf{M}(\mathbf{q})\ddot{\mathbf{q}} + \mathbf{C}(\mathbf{q}, \dot{\mathbf{q}})\dot{\mathbf{q}} + \mathbf{G}(\mathbf{q}) = \boldsymbol{\tau} \\ \boldsymbol{\tau} = \boldsymbol{\tau}_B + \boldsymbol{\tau}_S + \boldsymbol{\tau}_I + \boldsymbol{\tau}_N \end{cases} \quad (1)$$

where $\mathbf{M}(\mathbf{q})$, $\mathbf{C}(\mathbf{q}, \dot{\mathbf{q}})$, $\mathbf{G}(\mathbf{q})$ are the inertia matrix, the generalized Coriolis term, and the gravity dependent torque respectively. The sum of the torques applied at the two joints is represented by $\boldsymbol{\tau}$. More specifically, $\boldsymbol{\tau}_B$ refers to the bias torque, generated by a reference tilt angle between the body and the vertical axis and set to zero (Morasso et al., 2019; Asai et al., 2009; Suzuki et al., 2012). The terms $\boldsymbol{\tau}_S$ and $\boldsymbol{\tau}_I$ refer to the stiffness and intermittent control respectively. The first one is due to the muscles mechanical properties, which passively contribute to the stabilization of the body. Thus, $\boldsymbol{\tau}_S$ was modeled by a proportional and derivative contributes, as highlighted in the following:

$$\boldsymbol{\tau}_S = \begin{bmatrix} K_a q_1 + B_a \dot{q}_1 \\ K_h q_2 + B_h \dot{q}_2 \end{bmatrix} \quad (2)$$

81 where K_a and K_h model the stiffness at the ankle and the hip. B_a and B_h
82 account for the intrinsic damping properties of the muscles. Instead, $\boldsymbol{\tau}_I$ models
83 the active role of the CNS, since a pure passive mechanical component cannot
84 stabilize human stance (Morasso & Sanguineti, 2002).

In the DIP/VIP modeling framework (Morasso et al., 2019), the novel aspect was to apply the intermittent control only at the ankle joint while the hip coupled the lower body segment passively with the upper trunk, contributing to the stabilization by means of $\boldsymbol{\tau}_S$. Thus, a key element is the use of the VIP model to generate active motor commands. Indeed, for any multi-link mechanical structure, one can obtain the position of the COM, i.e. $x_g(\mathbf{q})$ and

$y_g(\mathbf{q})$ in figure 1 by computing its sway angle q_{COM} (Morasso et al., 2019). The active control τ_I can be computed following (Morasso et al., 2019; Asai et al., 2009):

$$\tau_I = \begin{cases} \begin{bmatrix} -(P\delta q_{COM} + D\delta \dot{q}_{COM}) \\ 0 \end{bmatrix} & \text{if } \delta q_{COM}(\delta \dot{q}_{COM} - \alpha \delta q_{COM}) > 0 \\ \begin{bmatrix} 0 \\ 0 \end{bmatrix} & \text{otherwise} \end{cases} \quad (3)$$

where δq_{COM} indicates q_{COM} delayed by δ interval of time used to model neural delay, fixed at $\delta = 0.2$ s (Morasso et al., 2019). The intermittent control law applies a proportional and derivative actions at the ankle joint whether COM leaves the stable manifold described by $\delta q_{COM}(\delta \dot{q}_{COM} - \alpha \delta q_{COM}) \leq 0$ (Asai et al., 2009). Here $\alpha = 0.4 \text{ s}^{-1}$ was chosen (Morasso et al., 2019; Asai et al., 2009). Conversely, active control switches off when the system approaches or remains in the stable manifold (Asai et al., 2009). Based on the results presented in (Morasso et al., 2019), in this work P varied between $0.3 \cdot mgh$ and $0.9 \cdot mgh$ $N \cdot m$, and D between 0 to 200 $N \cdot m \cdot s / rad$ (Morasso et al., 2019).

As reported by (Suzuki et al., 2012; Conforto et al., 2001), quiet upright stance is challenged not only by the gravity field, but also by internal postural noise (Asai et al., 2009; Conforto et al., 2001), represented by τ_N , which acts independently at the two joints. τ_N was modeled as white noise, low-pass filtered at 10 Hz and having standard deviation of 0.2 $N \cdot m$ (Morasso et al., 2019; Suzuki et al., 2012).

2.3. COP formulation for the double link inverted pendulum

Despite the plausibility of DIP/VIP model was assessed in reproducing kinematic human-like sway patterns, no hint regarding the COP time evolution was

given (Morasso et al., 2019). In the stance phase (see figure 1) the following equation holds (Chevallereau et al., 2008):

$$m \begin{bmatrix} \ddot{x}_g \\ \ddot{y}_g \end{bmatrix} + mg \begin{bmatrix} 0 \\ 1 \end{bmatrix} = \mathbf{R} = \begin{bmatrix} R_x \\ R_y \end{bmatrix} \quad (4)$$

where m is the total mass of the subject, g is the gravity acceleration, and \mathbf{R} represents the ground reaction force with its two components R_x and R_y . The equilibrium of the DIP around the ankle joint axis can be obtained as:

$$\dot{\sigma}_a = mgx_g - COP(t)R_y - l_a R_x \quad (5)$$

where σ_a is the angular momentum of the DIP about the ankle, COP is the displacement of the center of pressure with respect to the ankle joint and l_a is the height of the latter with respect to the ground (see figure 1). By definition, σ_a is linear with respect to the joint velocities and can be written as reported in (Chevallereau et al., 2008):

$$\sigma_a = \frac{\partial}{\partial \dot{q}_1} \mathcal{L}(\mathbf{q}, \dot{\mathbf{q}}) = \mathbf{N}(\mathbf{q}) \dot{\mathbf{q}} \quad (6)$$

σ_a is a conjugate momentum **that can be obtained by differentiating the Lagrangian** $\mathcal{L}(\mathbf{q}, \dot{\mathbf{q}})$ of the system with respect to \dot{q}_1 . Such derivative can be rearranged as the scalar product between the vector field $\mathbf{N}(\mathbf{q})$ and the joint velocity vector $\dot{\mathbf{q}}$ (Westervelt et al., 2018) (appendix). Combining (4) and (5), it is possible to compute the COP for a DIP structure:

$$COP(t) = \frac{mgx_g - (\dot{\sigma}_a + ml_a \ddot{x}_g)}{m(\ddot{y}_g + g)} \quad (7)$$

Since the product of l_a and R_x in (5) can be profiled out (Schut et al., 2020), this finally leads to:

$$COP(t) = \frac{mgx_g - \dot{\sigma}_a}{m(\ddot{y}_g + g)} \quad (8)$$

101 2.4. COP parameters selection and model evaluation

102 Three COP descriptors were used to assess the kinetic plausibility of the
 103 DIP/VIP model. Such descriptors were selected among a set of six, based on
 104 their ability in underlining significant differences between the two populations
 105 (Y and O). The initial feature set embraced the only two universal indexes in
 106 AP direction presented in (Yamamoto et al., 2015): the frequency at which
 107 COP presents the 50% (PF50) of its whole power spectrum density (PSD) (Ya-
 108 mamoto et al., 2015; Prieto et al., 1996), and the slope of the PSD in the low
 109 frequency band 0.1 - 0.5 Hz (SLOPE-L) (Asai et al., 2009; Yamamoto et al.,
 110 2015). Also the critical time (T_{CR}) was included (Toosizadeh et al., 2015; Ya-
 111 mamoto et al., 2015; Novak et al., 2009), obtained as the time interval at which
 112 the intersection between the two fitting lines on linear-scale stabilogram dif-
 113 fusion plot (SDP) occurs (Collins & De Luca, 1993). Finally, the generalized
 114 Hurst exponent (HE), computed through detrended fluctuation analysis (DFA)
 115 (Amoud et al., 2007; Srinivasan et al., 2012), was also considered, together with
 116 two features related to sway amplitude, i.e. the mean distance (MD) and the
 117 sway range (SR) (Prieto et al., 1996; Błaszczyk et al., 2007). For the DFA
 118 computation the windows size ranged from 0.1 s (10 samples) and 10 s (1000
 119 samples). Each feature was computed for both Y and O groups. Normality of
 120 data distributions was tested through the Kolmogorov-Smirnov test. Compar-
 121 isons between groups were performed by ANOVA or Wilcoxon rank sum test for
 122 gaussian or non-gaussian distributed data. For each test, statistical significance
 123 was set at $p < 0.05$.

124 PF50, T_{CR} and HE resulted able to discriminate between Y and O groups

and thus used for the evaluation of COP time-series obtained as output of the DIP/VIP. Such model was implemented in MATLAB/Simulink (The Mathworks Inc.). The anthropometric characteristics required to fill the model were computed as the average among the subjects (appendix). The ranges of values for P and D parameters (section 2.2) were linearly spaced forming a parameter space and used to parametrize the intermittent controller for the simulation of COP from the DIP/VIP model. **P-D grids representation was limited to those values for which the model provided stable and physiologically plausible outputs.** For each combination of P-D parameters, 10 COP time-series were generated.

Then, PF50, T_{CR} and HE were computed for each COP, providing the dependency of each metric upon P and D combinations. For both groups, it was assumed a plausible range for each considered metric (PMR), defined as the mean population value \pm standard deviation (Table 1). Eventually, a series of grids was built to obtain P and D ranges for which all the three COP descriptors were coherent with synthetic and real data at the same time. Therefore, those P-D values for which the feature maps fell within the PMR-Y and PMR-O at least one time among the ten COP realizations and for all of the three features were selected.

3. Results

The average PSD, represented in a log-log scale (figure 2a) shows a higher power content at the lower frequencies for the Y group and a statistically significant lower PF50 (figure 2b), as confirmed also by the PMR (Table 1).

For Y population, the mean SDP (figure 2c) increased less than the elderly at the lower time scales. This contributes to the higher T_{CR} (Table 1), since the SDP slope in its first part heavily impacts on the T_{CR} estimation (Collins & De Luca, 1993). The statistical analysis (figure 2d) showed significant differences

151 between the groups.

152 Eventually, the HE exhibited a strong significant difference between the two
 153 groups (figure 2f), confirming the discriminant power of this feature (Amoud
 154 et al., 2007). This can be appreciated also from the remarkable change in the
 155 average regression lines slope between Y and O groups (figure 2e and Table 1).

156 The three COP descriptors were also computed for the synthetic COP data.
 157 Gray-maps (figure 3) describe how PF50, T_{CR} and HE vary with respect to
 158 the active control parameterization. PF50 seems to be more sensitive to the
 159 variations of D when P was ≈ 300 N·m/rad (figure 3a), and greater PF50
 160 excursions were found for low P values. On the opposite, T_{CR} (figure 3b) seemed
 161 to better mirror changes in the P parameter when D was low (between 0 and 50
 162 N·m·s/rad). The HE instead presented a smoothed trend, radially decreasing
 163 when both P and D increase (figure 3c). Eventually, the ranges obtained for
 164 the two groups were reported in table 2 and their average \pm standard deviation
 165 values are reported as shaded areas in figure 3. Larger P and D values were
 166 admissible to obtain COP having characteristics in line with the O group with
 167 respect to the Y population. On the contrary, the Y group admitted narrower
 168 P and D ranges.

Table 1: Table shows PMR for the three parameters and for both populations.

Group	PMR		
	PF50 (Hz)	T_{CR} (s)	HE
Y	0.09 \pm 0.06	1.63 \pm 0.59	1.32 \pm 0.12
O	0.16 \pm 0.13	1.12 \pm 0.32	1.17 \pm 0.13

Table 2: Table shows the considered P and D ranges for the grids.

Group	P (N·m/rad)	D (N·m·s/rad)
Y	257.36÷322.38	0÷49.47
O	257.36÷463.25	0÷74.21

169 4. Discussion

170 The P-D grids (figure 3) seemed to confirm not only the sensitivity of syn-
171 thetic COP to different parameterizations of the active controller, but also the
172 possibility to obtain time-series whose descriptors lie within the PMR observed
173 in the Y and O groups. This supports the goodness of the DIP/VIP model for
174 the description of the human stance from a kinetic perspective, in addition to
175 the kinematic one (Morasso et al., 2019).

176 Further, both P and D admitted greater values for the O group compared
177 to the Y one (Table 2). This might indicate the well known functional rear-
178 rangement of the CNS control recognized in the elderly (Allum et al., 2002;
179 Collins et al., 1995), which can be mapped through the tuning of the intermit-
180 tent controller and mirrored by the COP. In passing, greater P and D values
181 were associated with lower HE in the O group (figure 3c). This aspect high-
182 lights an enhanced anti-persistent behavior of the elderly, aligning with (Amoud
183 et al., 2007; Collins et al., 1995) and indicating that greater regulatory efforts
184 are needed to achieve stability (Collins et al., 1995), resulting in a more ener-
185 getically expensive control (Asai et al., 2009).

186 Regarding the PF50, it quantifies the spreading of the COP spectrum to-
187 wards the higher frequencies, i.e. the greater is the PF50, the larger is the
188 amount of power of faster dynamics, possibly associated with an augmented
189 level of stochasticity (Yamamoto et al., 2015; Collins & De Luca, 1993). Since

190 COP encompasses control torques at the lower limbs joints, it undoubtedly re-
 191 flects also motor commands modulated by muscles activity and their mechanical
 192 characteristics (Baratto et al., 2002). Therefore, an enhanced stochastic COP
 193 behavior might refer to a “stiffer” muscular strategy, recognizable in the elderly
 194 (Collins et al., 1995) and associated either to mechanical muscles properties or
 195 to neuromodulatory changes. A global sign of this phenomenon can be found
 196 in the PSD slope at the lower frequencies (SLOPE-L) (Yamamoto et al., 2015;
 197 Suzuki et al., 2020; Asai et al., 2009): a nearly flat slope points out a body stiff-
 198 ness which tends to be overcritical, i.e. $\gg mgh$, while a negative value stands
 199 for an optimal stiffness tuning and thus an efficient regulation (Suzuki et al.,
 200 2020; Asai et al., 2009). The former case was associated to a continuous control
 201 with higher gains (Asai et al., 2009), while the latter takes advantages from a
 202 VSC policy to achieve the global stabilization, admitting lower control gains,
 203 resembling a physiological plausible dynamic (Morasso et al., 2019; Suzuki et al.,
 204 2020). This agrees with the greater P values for the O population and is also
 205 supported by the SLOPE-L computed on the real data of both groups: as ex-
 206 pected they resulted higher for the O subjects (-0.95 ± 0.84) with respect to the
 207 Y ones (-1.62 ± 1.15).

208 Eventually, the T_{CR} appears less sensitive to changes in the P-D parame-
 209 ters. From the grids (figure 3b) it is easy to appreciate that T_{CR} has a uniform
 210 trend and limited variations for a large set of the controller parameterizations.
 211 This aspect is not completely surprising. Despite the DIP/VIP represents a
 212 highly descriptive model of the human stance, it naturally incorporates some
 213 approximations. Thus, the T_{CR} and the SDP appear able to highlight subtle
 214 properties of balance, which might not be necessarily exploited by a mechanistic
 215 model, whenever accurate (Baratto et al., 2002). In addition, the SDP repre-
 216 sents a conceptual framework for analyzing sway data, grounded on a timeseries

217 perspective rather than on a biomechanical modeling of the system generating
 218 COP data (Collins & De Luca, 1993; Baratto et al., 2002). Thus, the role of the
 219 T_{CR} in describing VSC models of posture deserves to be further investigated,
 220 since it showed to be highly descriptive of different control dynamics exhibited in
 221 both healthy individuals and populations presenting a wide spectrum of balance
 222 disorders (Toosizadeh et al., 2015; Novak et al., 2009). **Note that the choice of a**
 223 **set of COP features already successfully used for investigating COP timeseries**
 224 **in young and elderly subjects (Amoud et al., 2007; Collins et al., 1995; Prieto**
 225 **et al., 1996) further supports the validity of the DIP/VIP model from a kinetic**
 226 **viewpoint. Eventually, it deserves to be mentioned that the active controller**
 227 **parameters investigation was limited to P and D gains, while α was set at a**
 228 **fixed value (Section 2.2). This could represent a partial limitation of the study,**
 229 **since the exploration of α in conjunction with P and D would add significant**
 230 **information regarding the model and thus it needs to be adequately examined**
 231 **in focused studies.**

232 Modern posturography highlighted the tendency to infer active controller
 233 parameters to underline differences among many populations or to identify a
 234 model for each subject (Suzuki et al., 2020; McKee & Neale, 2019). This is
 235 commonly achieved using data or features derived from COM, even if COP
 236 measures were the most common data used in classical posturography (Morasso
 237 et al., 2019; Suzuki et al., 2012; Morasso, 2020). However, at least a couple of
 238 aspects suggest the opportunity to use COP rather than COM. Firstly, COP is a
 239 directly measurable quantity, while the COM can only be estimated in a variety
 240 of different ways, including the direct computation from COP, which results into
 241 a smoothed version of the latter (Morasso et al., 1999; Eng & Winter, 1993).
 242 Despite such procedures are commonly employed to highlight kinesiological fea-
 243 tures of balance, they could lead to a loss of information, that can be instead

244 captured through different identification approaches (Suzuki et al., 2020; Cor-
 245 radini et al., 1997). Indeed, the COP trajectory represents a meaningful source
 246 of information regarding both the descending neural control and the mechan-
 247 ical actuation provided by the musculoskeletal system (Baratto et al., 2002),
 248 appearing a more preferable choice when human stance is investigated from a
 249 neuromuscular perspective. However, the use of a multi-link structure renders
 250 more challenging the COP modeling, while defining COP from a single-link in-
 251 verted pendulum is quite straightforward (Schut et al., 2020). In this view,
 252 the relation (8) (section 2.3) can be employed for double-link models. Thus,
 253 despite the identification was not the aim of this study, the COP formulation
 254 here developed represents itself a valuable contribution toward the integration of
 255 physiological data and mechanical models of balance, since the latter provide a
 256 high interpretability of its parameters, which can be linked to specific properties
 257 of the neuromuscular system.

258 The additional value of using a DIP/VIP or in general a multi-link model
 259 can be appreciated also considering that this allows to investigate if changes in
 260 neural control are reflected in how CNS manages the intrinsic body redundancy
 261 of the quiet stance (Suzuki et al., 2012; Reimann & Schöner, 2017). Indeed, a
 262 loss of the CNS capacity in efficiently managing the redundancy can be a sign
 263 of a functional rearrangement due to neurological disorders (Corradini et al.,
 264 1997). The central role of COP in accounting for mechanical redundancy is
 265 fundamental also in other applications, e.g. bipedal legged robotics. In this
 266 context, the COP and more in general the zero moment point has to encompass
 267 the multi-link structure in its formulation, in order to properly control both
 268 the standing and dynamic phases of gait (Chevallereau et al., 2008; Westervelt
 269 et al., 2018). Therefore, an inefficient regulatory activity can be mirrored, and
 270 thus recognized, by considering COP characteristics (Peterka, 2009). This could

271 hold also for the human system, where a degraded regulatory activity, due to
272 disease, can affect the multi-link structure management in balance maintenance,
273 which is *per se* a redundant motor task (Reimann & Schöner, 2017).

274 These aspects support the findings of Morasso et al. (2019), enriched in this
275 study by the kinetic perspective. Present results highlight the suitability of
276 modeling balance through a DIP structure, where VSC accounts for the CNS
277 role. The hybrid policy is employed for managing the body redundancy through
278 the VIP part of the model and resulted to drive synthetic COP characteristics.
279 Indeed, since a physiological coherent model of the control action at the two
280 joints was employed, human-like patterns were observed in the simulated COP
281 time-series. As emerged from (8) and (17), COP spans non linearly the torque
282 vector τ over σ_a . Thus, both passive and active effects at the hip and ankle
283 were mirrored in the COP, which lumps the information about the stability of
284 the structure.

285 A further consideration regards the importance of a proper COP modeling,
286 since COP can be used as a feedback information in the balance control loop
287 (Peterka, 2009), rendering the system robust with respect to external perturba-
288 tions, e.g. support base movements or external impacts (Peterka, 2009; Prahlad
289 et al., 2008). Note that also quiet stance undergoes internal and external distur-
290 bance (Conforto et al., 2001; Nomura et al., 2013) and thus COP represents itself
291 a valuable source of information that can be used by the CNS for tuning bal-
292 ance control strategies in either perturbed or unperturbed conditions. Despite
293 one can wonder about the existence of an internal model of the COP within
294 the CNS (Morasso et al., 2019), there is no doubt regarding the existence of
295 an integration process of tactile and proprioceptive sensors of the feet (Viseux,
296 2020), that makes plausible the existence of COP information within the balance
297 control schemes (Morasso et al., 2019). This suggests a more profound picture

298 regarding the nature of the COP. Indeed, as for certain balancing tasks, CNS
 299 must switch the role between COP and COM information in the motor control
 300 paradigm (Morasso, 2020). Thus, although classical literature (Winter, 2009)
 301 agreed in viewing the COM as the controlled variable and COP as the control
 302 variable, it could be a limiting assumption for studying possible rearrangements
 303 in the motor control with respect to neurological disorders. This aspect can be
 304 further investigated in future studies, where kinematic and kinetic simultaneous
 305 measures are available (Santos & Duarte, 2016), in order to better clarify the
 306 relationship between COP and COM in this kind of modeling framework.

307 Appendix

In this section further details regarding the dynamical equation (1), as well as
 a clarification on the conjugate momentum presented in (6) are shown. Consider
 the double-link inverted pendulum given in figure 1. By means of Lagrangian
 formulation, one can easily obtain the matrices required in (1) (Siciliano et al.,
 2010; Morasso et al., 2019). In particular:

$$\mathbf{M}(\mathbf{q}) = \begin{bmatrix} M_{11} & M_{12} \\ M_{21} & M_{22} \end{bmatrix} \quad (9)$$

$$\mathbf{C}(\mathbf{q}, \dot{\mathbf{q}}) = \begin{bmatrix} C_{11} & C_{12} \\ C_{21} & 0 \end{bmatrix} \quad (10)$$

$$\mathbf{G}(\mathbf{q}) = -g \begin{bmatrix} G_1 \\ G_2 \end{bmatrix} \quad (11)$$

where

$$\begin{cases} M_{11} = I_1 + I_2 + m_1 l_1^2 + m_2 (L^2 + l_2^2 + 2Ll_2 \cos q_2) \\ M_{12} = M_{21} = I_2 + m_2 (l_2^2 + Ll_2 \cos q_2) \\ M_{22} = I_2 + m_2 l_2^2 \end{cases} \quad (12)$$

$$\begin{cases} C_{11} = -m_2 Ll_2 \dot{q}_2 \sin q_2 \\ C_{12} = -m_2 Ll_2 (\dot{q}_1 + \dot{q}_2) \sin q_2 \\ C_{21} = m_2 Ll_2 \dot{q}_2 \sin q_2 \end{cases} \quad (13)$$

$$\begin{cases} G_1 = (m_1 l_1 + m_2 L) \sin q_1 + m_2 l_2 \sin(q_1 + q_2) \\ G_2 = m_2 l_2 \sin(q_1 + q_2) \end{cases} \quad (14)$$

Regarding the conjugate momentum of the DIP with respect to the ankle joint σ_a (equation (6)), **it can be obtained differentiating** the Lagrangian with respect to the generalized velocity \dot{q}_1 . Consider the Lagrangian of the mechanical system:

$$\mathcal{L}(\mathbf{q}, \dot{\mathbf{q}}) := \mathcal{K}(\mathbf{q}, \dot{\mathbf{q}}) - \mathcal{V}(\mathbf{q}) \quad (15)$$

where the first two terms express the total kinetic and potential energy of the system, respectively (Siciliano et al., 2010; Westervelt et al., 2018). Then, one can observe that only $\mathcal{K}(\mathbf{q}, \dot{\mathbf{q}})$ depends on the generalized velocity $\dot{\mathbf{q}}$. From this, it directly follows that:

$$\sigma_a := \frac{\partial}{\partial \dot{q}_1} \mathcal{K}(\mathbf{q}, \dot{\mathbf{q}}) \quad (16)$$

which is convenient since one can observe that:

$$\sigma_a = \begin{bmatrix} M_{11} & M_{12} \end{bmatrix} \dot{\mathbf{q}} = \mathbf{N}(\mathbf{q}) \dot{\mathbf{q}} \quad (17)$$

By differentiating the last equation with respect to time, it follows that the term $\ddot{\mathbf{q}}$ appears in the derivative, which is proportional to the control torques, through the dynamic equation of the DIP (equation (1)). Thus, it follows that all the mechanical fluctuations at the joints are spanned over the COP by $\dot{\sigma}_a$. For supplementary details the reader can refer to (Siciliano et al., 2010; Westervelt et al., 2018). Finally, Table 3 reports the anthropometric characteristics, derived following the relations in (Winter, 2009), of the mean population used to fill the DIP/VIP model.

Table 3: Table shows the anthropometric values used to fill the DIP/VIP model in the simulation steps.

L	l_1	l_2	m_1	m_2	I_1	I_2	K_a	K_h	B_a	B_h
(m)	(m)	(m)	(kg)	(kg)	(kg·m ²)	(kg·m ²)	(N·m/rad)	(N·m/rad)	(N·m·s/rad)	(N·m·s/rad)
0.87	0.39	0.45	19.3	40.7	2.9	7.9	366.0	246.0	22.0	22.0

315

316 Conflict of interest statement

317 The authors declare that there is no conflict of interest.

318 References

- 319 Allum, J., Carpenter, M., Honegger, F., Adkin, A., & Bloem, B. (2002). Age-
320 dependent variations in the directional sensitivity of balance corrections and
321 compensatory arm movements in man. *The Journal of Physiology*, 542, 643–
322 663.
- 323 Amoud, H., Abadi, M., Hewson, D. J., Michel-Pellegrino, V., Doussot, M., &
324 Duchêne, J. (2007). Fractal time series analysis of postural stability in elderly
325 and control subjects. *Journal of Neuroengineering and Rehabilitation*, 4, 12.

326 Aramaki, Y., Nozaki, D., Masani, K., Sato, T., Nakazawa, K., & Yano, H.
327 (2001). Reciprocal angular acceleration of the ankle and hip joints during
328 quiet standing in humans. *Experimental Brain Research*, 136, 463–473.

329 Asai, Y., Tasaka, Y., Nomura, K., Nomura, T., Casadio, M., & Morasso, P.
330 (2009). A model of postural control in quiet standing: robust compensation
331 of delay-induced instability using intermittent activation of feedback control.
332 *PLoS One*, 4, e6169.

333 Baratto, L., Morasso, P. G., Re, C., & Spada, G. (2002). A new look at postur-
334 ographic analysis in the clinical context: sway-density versus other parame-
335 terization techniques. *Motor Control*, 6, 246–270.

336 Błaszczyk, J., Orawiec, R., Duda-Kłodowska, D., & Opala, G. (2007). Assess-
337 ment of postural instability in patients with parkinson’s disease. *Experimental*
338 *Brain Research*, 183, 107–114.

339 Cardarelli, S., Mengarelli, A., Tigrini, A., Strazza, A., Di Nardo, F., Fioretti,
340 S., & Verdini, F. (2019). Single imu displacement and orientation estimation
341 of human center of mass: A magnetometer-free approach. *IEEE Transactions*
342 *on Instrumentation and Measurement*, 69, 5629–5639.

343 Casadio, M., Morasso, P. G., & Sanguineti, V. (2005). Direct measurement of
344 ankle stiffness during quiet standing: implications for control modelling and
345 clinical application. *Gait & Posture*, 21, 410–424.

346 Cenciarini, M., Loughlin, P. J., Sparto, P. J., & Redfern, M. S. (2010). Stiffness
347 and damping in postural control increase with age. *IEEE Transactions on*
348 *Biomedical Engineering*, 57, 267–275.

349 Chevallereau, C., Djoudi, D., & Grizzle, J. W. (2008). Stable bipedal walking

350 with foot rotation through direct regulation of the zero moment point. *IEEE*
351 *Transactions on Robotics*, 24, 390–401.

352 Collins, J., De Luca, C., Burrows, A., & Lipsitz, L. (1995). Age-related changes
353 in open-loop and closed-loop postural control mechanisms. *Experimental*
354 *Brain Research*, 104, 480–492.

355 Collins, J. J., & De Luca, C. J. (1993). Open-loop and closed-loop control of pos-
356 ture: a random-walk analysis of center-of-pressure trajectories. *Experimental*
357 *Brain Research*, 95, 308–318.

358 Conforto, S., Schmid, M., Camomilla, V., D’Alessio, T., & Cappozzo, A. (2001).
359 Hemodynamics as a possible internal mechanical disturbance to balance. *Gait*
360 *& Posture*, 14, 28–35.

361 Corradini, M. L., Fioretti, S., Leo, T., & Piperno, R. (1997). Early recognition
362 of postural disorders in multiple sclerosis through movement analysis: a mod-
363 eling study. *IEEE Transactions on Biomedical Engineering*, 44, 1029–1038.

364 Eng, J., & Winter, D. (1993). Estimations of the horizontal displacement of the
365 total body centre of mass: considerations during standing activities. *Gait &*
366 *Posture*, 1, 141–144.

367 McKee, K. L., & Neale, M. C. (2019). Direct estimation of the parameters of a
368 delayed, intermittent activation feedback model of postural sway during quiet
369 standing. *PloS one*, 14, e0222664.

370 Milton, J., & Insperger, T. (2019). Acting together, destabilizing influences can
371 stabilize human balance. *Philosophical Transactions of the Royal Society A*,
372 377, 20180126.

373 Morasso, P. (2020). Centre of pressure versus centre of mass stabilization strate-
374 gies: the tightrope balancing case. *Royal Society Open Science*, 7, 200111.

375 Morasso, P., Cherif, A., & Zenzeri, J. (2019). Quiet standing: The single in-
376 verted pendulum model is not so bad after all. *PloS One*, *14*, e0213870.

377 Morasso, P. G., & Sanguineti, V. (2002). Ankle muscle stiffness alone cannot
378 stabilize balance during quiet standing. *Journal of neurophysiology*, *88*, 2157–
379 2162.

380 Morasso, P. G., Spada, G., & Capra, R. (1999). Computing the com from the
381 cop in postural sway movements. *Human Movement Science*, *18*, 759–767.

382 Nomura, T., Oshikawa, S., Suzuki, Y., Kiyono, K., & Morasso, P. (2013). Mod-
383 eling human postural sway using an intermittent control and hemodynamic
384 perturbations. *Mathematical Biosciences*, *245*, 86–95.

385 Novak, V., Haertle, M., Zhao, P., Hu, K., Munshi, M., Novak, P., Abduljalil, A.,
386 & Alsop, D. (2009). White matter hyperintensities and dynamics of postural
387 control. *Magnetic Resonance Imaging*, *27*, 752–759.

388 Peterka, R. J. (2000). Postural control model interpretation of stabilogram
389 diffusion analysis. *Biological Cybernetics*, *82*, 335–343.

390 Peterka, R. J. (2009). Comparison of human and humanoid robot control of
391 upright stance. *Journal of Physiology-Paris*, *103*, 149–158.

392 Popović, M. B. (2013). *Biomechanics and robotics*. CRC Press.

393 Prahlad, V., Dip, G., & Meng-Hwee, C. (2008). Disturbance rejection by online
394 zmp compensation. *Robotica*, *26*, 9.

395 Prieto, T. E., Myklebust, J. B., Hoffmann, R. G., Lovett, E. G., & Myklebust,
396 B. M. (1996). Measures of postural steadiness: differences between healthy
397 young and elderly adults. *IEEE Transactions on Biomedical Engineering*, *43*,
398 956–966.

- 399 Reimann, H., & Schöner, G. (2017). A multi-joint model of quiet, upright stance
400 accounts for the “uncontrolled manifold” structure of joint variance. *Biological*
401 *Cybernetics*, 111, 389–403.
- 402 Santos, D. A., & Duarte, M. (2016). A public data set of human balance
403 evaluations. *PeerJ*, 4, e2648. doi:10.7717/peerj.2648.
- 404 Schut, I., Pasma, J., Roelofs, J., Weerdesteyn, V., van der Kooij, H., &
405 Schouten, A. (2020). Estimating ankle torque and dynamics of the stabi-
406 lizing mechanism: no need for horizontal ground reaction forces. *Journal of*
407 *Biomechanics*, (p. 109813).
- 408 Siciliano, B., Sciavicco, L., Villani, L., & Oriolo, G. (2010). *Robotics: modelling,*
409 *planning and control*. Springer Science & Business Media.
- 410 Srinivasan, B., Spinner, T., & Rengaswamy, R. (2012). Control loop perfor-
411 mance assessment using detrended fluctuation analysis (dfa). *Automatica*,
412 48, 1359–1363.
- 413 Suzuki, Y., Nakamura, A., Milosevic, M., Nomura, K., Tanahashi, T., Endo,
414 T., Sakoda, S., Morasso, P., & Nomura, T. (2020). Postural instability via a
415 loss of intermittent control in elderly and patients with parkinson’s disease: A
416 model-based and data-driven approach. *Chaos: An Interdisciplinary Journal*
417 *of Nonlinear Science*, 30, 113140.
- 418 Suzuki, Y., Nomura, T., Casadio, M., & Morasso, P. (2012). Intermittent control
419 with ankle, hip, and mixed strategies during quiet standing: a theoretical
420 proposal based on a double inverted pendulum model. *Journal of Theoretical*
421 *Biology*, 310, 55–79.
- 422 Toosizadeh, N., Mohler, J., Armstrong, D. G., Talal, T. K., & Najafi, B. (2015).

423 The influence of diabetic peripheral neuropathy on local postural muscle and
424 central sensory feedback balance control. *PloS One*, 10, e0135255.

425 Viseux, F. J. (2020). The sensory role of the sole of the foot: Review and update
426 on clinical perspectives. *Neurophysiologie Clinique*, 50, 55–68.

427 Westervelt, E. R., Grizzle, J. W., Chevallereau, C., Choi, J. H., & Morris, B.
428 (2018). *Feedback control of dynamic bipedal robot locomotion*. CRC press.

429 Winter, D. A. (2009). *Biomechanics and motor control of human movement*.
430 John Wiley & Sons.

431 Yamamoto, T., Smith, C. E., Suzuki, Y., Kiyono, K., Tanahashi, T., Sakoda, S.,
432 Morasso, P., & Nomura, T. (2015). Universal and individual characteristics
433 of postural sway during quiet standing in healthy young adults. *Physiological*
434 *Reports*, 3, e12329.

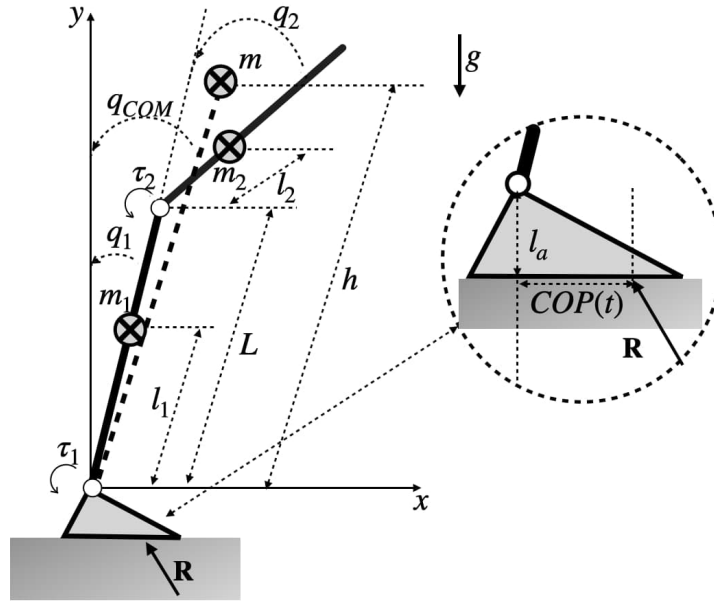


Figure 1: Schematic representation of the human upright stance through a double inverted pendulum (DIP) and its induced single link inverted pendulum model (VIP). The latter virtually links the center of mass COM with the ankle joint.

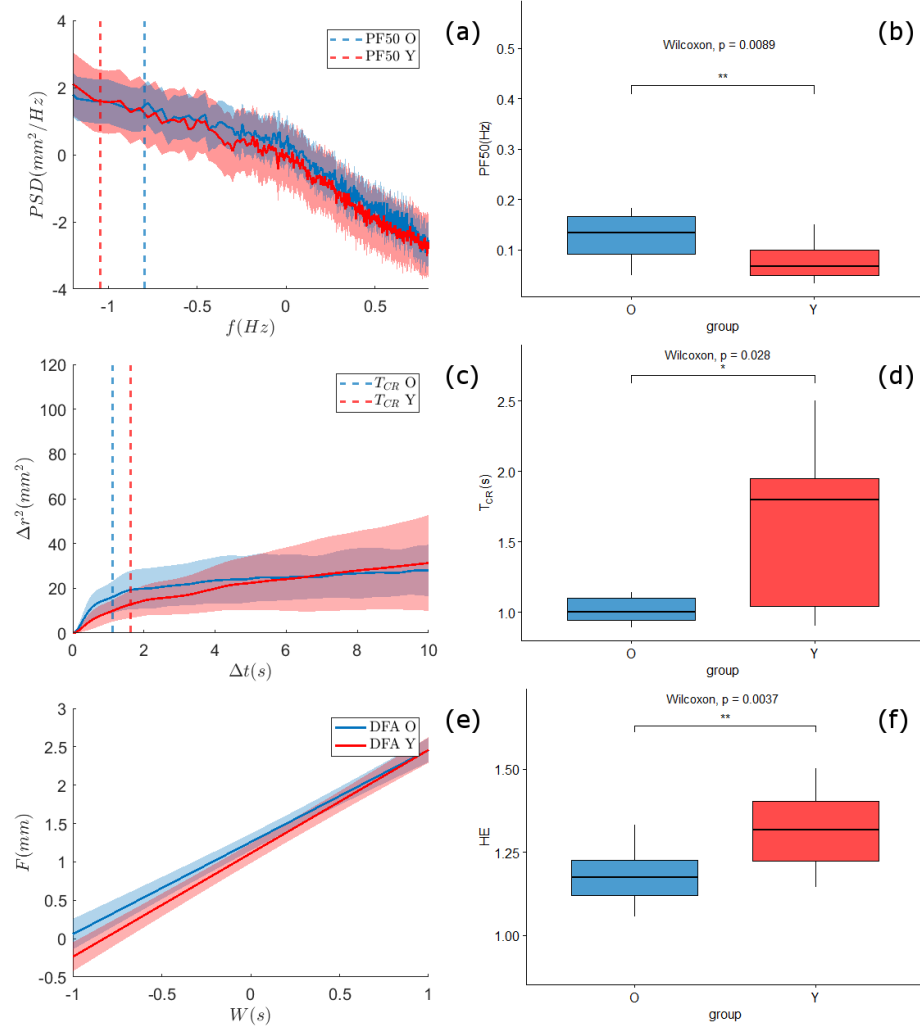


Figure 2: Left panels (2a, 2c) show PSD and SDP averaged values for Y (red) and O (blue) populations. Standard deviations are represented by shaded areas. In panel 2a, vertical dashed lines indicate mean PF50 values for both groups. Vertical dashed lines in panel 2a and 2c represent respectively mean PF50 and mean T_{CR} for Y and O groups. The average regression lines obtained from DFA analysis are presented in panel 2e. Shaded areas stand for the standard deviations. In panels 2a and 2e, both axes are expressed in common logarithmic scale. Right panels (2b, 2d, 2f) show Y (red) and O (blue) groups comparisons for PF50, T_{CR} : and HE. ** indicates $p < 0.01$ and * stands for $p < 0.05$.

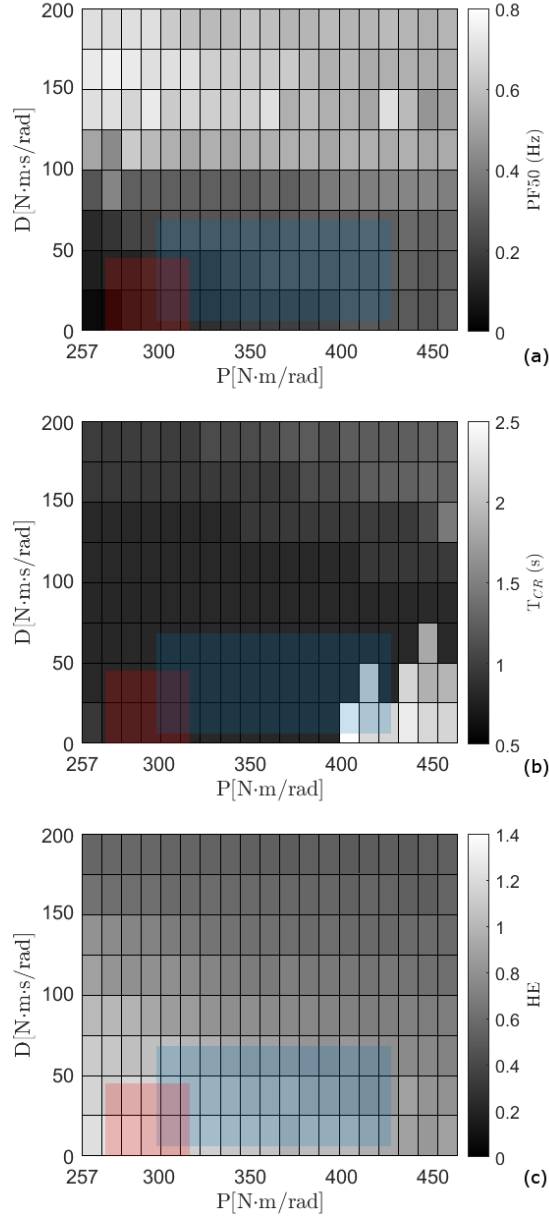


Figure 3: Panel 3a shows how PF_{50} varied with respect to the P and D parameters. Color-map was obtained computing PF_{50} from the synthetic COP time-series, obtained for each point of the P-D grid. T_{CR} and HE were computed with the same line and shown in panel 3b and 3c respectively. Shaded boxes, for Y (red) and O (blue) populations, are centered in the average P-D values ($289.9 - 24.7$ for Y and $360.3 - 37.1$ for O), while the areas account for the standard deviation ($23.4 - 20.1$ for Y and $64.1 - 31.9$ for O).